

## Quantum Computers Based on Electron Spins Controlled by Ultrafast Off-Resonant Single Optical Pulses

Susan M. Clark,<sup>1,\*</sup> Kai-Mei C. Fu,<sup>1</sup> Thaddeus D. Ladd,<sup>1,2</sup> and Yoshihisa Yamamoto<sup>1,2</sup>

<sup>1</sup>*Edward L. Ginzton Laboratory, Stanford University, Stanford, California 94305-4088, USA*

<sup>2</sup>*National Institute of Informatics, 2-1-2 Hitotsubashi, Chiyoda-ku, Tokyo 101-8430, Japan*

(Received 17 October 2006; revised manuscript received 13 May 2007; published 23 July 2007)

We describe a fast quantum computer based on optically controlled electron spins in charged quantum dots that are coupled to microcavities. This scheme uses broadband optical pulses to rotate electron spins and provide the clock signal to the system. Nonlocal two-qubit gates are performed by phase shifts induced by electron spins on laser pulses propagating along a shared waveguide. Numerical simulations of this scheme demonstrate high-fidelity single-qubit and two-qubit gates with operation times comparable to the inverse Zeeman frequency.

DOI: [10.1103/PhysRevLett.99.040501](https://doi.org/10.1103/PhysRevLett.99.040501)

PACS numbers: 03.67.Lx, 32.80.Qk, 33.35.+r, 42.65.Re

Quantum computers potentially allow improvement in computational speed over existing computers if an architecture is found with a fast clock rate and the ability to be scaled to many qubits and operations [1]. Electron spins of charged semiconductor quantum dots are promising candidates for such an architecture because of their potential integration into existing microtechnology. Most proposals for electron-spin quantum computers [2–5], however, restrict logic operations to nearest neighbors, limiting the computational clock rate. Optically mediated quantum logic [6–9] for two-qubit gates and fast single-qubit rotations [10,11] may improve the overall clock rate of the system.

Several previous works suggest techniques for fast single-qubit rotations of electron spins. Ground-state coherence generation via ultrafast pulses in molecular, atomic, and quantum-dot spectroscopy [11–16] indicates the ability to control ground-state populations and phases. This control is faster than that of microwave pulses or multiple, adiabatic narrow-band optical pulses. The application of ultrafast pulses to U(1) control of single quantum-dot qubits has been proposed [10]. Here we describe complete optical SU(2) control of single dots using similar techniques.

There are also proposals for optically mediated entanglement formation between two nonlocal qubits. One type of proposal uses coherently generated single photons [9,17], but requires precisely shaped optical pulses. Recent methods for the entanglement of atomic ensembles via simple optical pulses [18,19] have led to proposals for optically mediated two-qubit gates based on small phase shifts of light via single qubits in cavities [8]. These latter techniques may be easier and faster than the use of coherently generated single photons. Here, we propose a unique way to combine both fast SU(2) single-qubit rotations and fast optically mediated two-qubit gates on a single semiconductor chip. These elements may lead toward the fastest potentially scalable quantum computing scheme of which the authors are aware.

Figure 1 shows a key component of such an architecture. It is a square millimeter of a semiconductor chip patterned with cavities. Each cavity holds a single-charged quantum dot and is connected to other cavities through a switched circular waveguide. Each quantum dot can be individually addressed by focused optical pulses incident perpendicular to the plane of the chip to perform single-qubit rotations. These pulses are part of a pulse train that serves as the system clock and could be supplied by a semiconductor mode-locked laser [20]. Pulses in the plane of the chip couple distant qubits, forming a “quantum bus” or “qubus,” which is the foundation of a two-qubit gate.

We now examine each aspect of this scheme in more detail. The dots themselves are single-charged, large-area quantum dots (e.g., InGaAs). Such dots are strong candidates for this architecture because they readily form the three-level  $\Lambda$  system necessary for stimulated Raman transitions [Fig. 2(a)] and they have the large oscillator strengths [21] necessary for fast spin rotations. The two lower states of this system are the electron Zeeman states and are split by a magnetic field applied along the  $z$  direction, which is perpendicular to the growth axis. The excited state consists of two electrons in a spin-singlet and a hole. The large heavy-hole–light-hole splitting allows us to neglect states from the light-hole excitons and describe the exciton angular-momentum states in the  $x$  basis:  $|m_h = \pm 3/2\rangle_x$ . If we apply  $\sigma^+$ -polarized light to the system, the two electron-spin states, denoted  $|0\rangle$  and  $|1\rangle$ , are coupled to

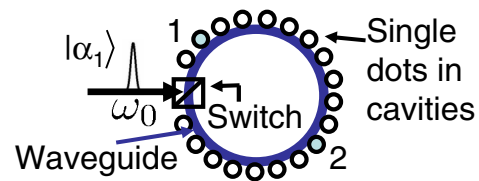


FIG. 1 (color online). Sketch of a loop-qubus quantum computer. The switch introduces, ejects, and provides displacement operations on the coherent-state pulse.

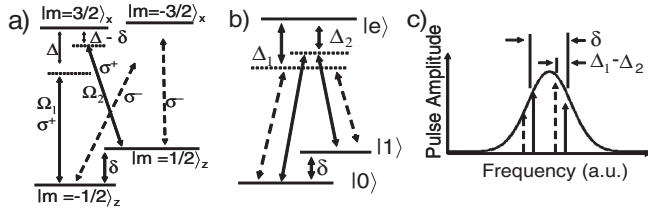


FIG. 2. (a) Energy level diagram for a charged quantum dot in an in-plane  $B$  field. Light with  $\sigma^+$  polarization incident along the growth direction ( $x$  axis) couples the  $|m_e = +1/2\rangle_x = 1/\sqrt{2}(|m_e = 1/2\rangle_z + |m_e = -1/2\rangle_z) \leftrightarrow |m_h = +3/2\rangle_x$  transitions, isolating a three-level system. (b) Energy level picture of two pairs of frequencies contained within the applied pulse that will induce transitions between states  $|0\rangle$  and  $|1\rangle$ . (c) Frequency domain picture of the optical pulse, showing the two pairs of frequency components shown in (b).

each other through the single  $|m_h = +3/2\rangle_x$  state, denoted  $|e\rangle$  [Fig. 2(a) and 2(b)].

Both single-qubit and two-qubit gates can be understood from the rotating-frame Hamiltonian

$$H = \delta P_1 + \Delta P_e + \sum_{j=0,1} \left[ \frac{\Omega_j(t)}{2} \sigma_j^+ + \frac{\Omega_j^\dagger(t)}{2} \sigma_j^- \right], \quad (1)$$

where  $P_j = |j\rangle\langle j|$  is the projection operator for  $|j\rangle$  and  $\sigma_j^+ = |e\rangle\langle j|$  is the raising operator for  $|j\rangle$ . Referring to Fig. 2,  $\delta$  is the ground-state splitting and  $\Delta$  is the detuning of the center frequency of the light pulse from  $\omega_0$ , the frequency of the  $|0\rangle \rightarrow |e\rangle$  transition. The meaning of the Rabi frequency  $\Omega_j(t)$  differs in the analyses of single- and two-qubit gates. For single-qubit gates, the intense light pulse perpendicular to the cavity is treated as a classical field and  $\Omega_j(t)$  is the product of the dipole matrix element and the time-dependent electric field amplitude of the light. For two-qubit gates, a weak coherent state of light interacts with the quantum dot in the single-mode cavity and  $\Omega_j(t)$  is a time-dependent Jaynes-Cummings coupling parameter multiplied by the cavity-photon annihilation operator  $a$ . There are also incoherent dynamics to be included in the time evolution of the system, so that the total time evolution is governed by the master equation

$$\dot{\rho} = -i[H, \rho] - \frac{\Gamma}{2} \left( P_e \rho + \rho P_e - \sum_{j=0,1} \sigma_j^- \rho \sigma_j^+ \right) - \frac{1}{T_2} (P_1 \rho P_0 + P_0 \rho P_1). \quad (2)$$

Here,  $\Gamma$  is the spontaneous emission rate of state  $|e\rangle$  and  $T_2$  is the electron-spin decoherence rate.

An approximation of the solutions of this equation may be found by the adiabatic elimination of the excited state, which is valid when the detuning  $\Delta$  is much larger than all other rates in the system. The three-level system is then reduced to a two-level spin system with effective Hamiltonian  $H_{\text{eff}} = G - \mathbf{B}_{\text{eff}} \cdot \mathbf{S}$ , where  $\mathbf{S}$  is the spin operator of the electron,  $G$  generates an irrelevant overall

phase, and the effective field is approximately

$$B_{\text{eff}}^z = -\delta + \frac{\Delta[\Omega_1^\dagger \Omega_1 - \Omega_0^\dagger \Omega_0] + \delta \Omega_0^\dagger \Omega_0}{4\Delta^2 + \Gamma^2}, \quad (3)$$

$$B_{\text{eff}}^x - iB_{\text{eff}}^y = -2 \frac{\Delta}{4\Delta^2 + \Gamma^2} \Omega_1^\dagger \Omega_0. \quad (4)$$

For simplicity, we consider a symmetric  $\Lambda$  system with  $\Omega_0 = \Omega_1$ , in which case  $B_{\text{eff}}^y = 0$ . Small deviations from this condition may alter the direction of  $\mathbf{B}_{\text{eff}}$  during the pulse, but they do not adversely affect the overall scheme.

For single-spin rotations in which short, intense, highly frequency detuned pulses are used, the effective field can be much larger than the applied magnetic field; i.e., the effective Rabi frequency  $|\Omega_{\text{eff}}| = \sqrt{4\Delta^2|\Omega_1|^4/(4\Delta^2 + \Gamma^2)^2 + \delta^2} \approx |\Omega_1|^2/2\Delta$  is much faster than the Larmor frequency. The rotation axis is determined by the phase difference between frequency components that are separated by the Zeeman frequency within the pulse spectrum [Fig. 2(b) and 2(c)] and thus by the delay time of the pulse with respect to clock intervals occurring with period  $2\pi/\delta$ . To see this, imagine that the spin precesses at Larmor frequency  $\delta$  for a time  $\phi/\delta$ , at which point an intense, broadband pulse is applied that rotates it through an angle  $\theta$  about  $\mathbf{B}_{\text{eff}}$ , which is approximately in the  $\hat{x}$  direction. Then, the spin freely precesses again for a time  $(2\pi - \phi)/\delta$ . This sequence can be written as the unitary operator

$$U = \exp[i\phi S_z] \exp[-i\theta S_x] \exp[i(2\pi - \phi) S_z] = -\exp[-i\theta(S_x \cos\phi - S_y \sin\phi)], \quad (5)$$

which describes a rotation with an axis determined by  $\phi$ . Pulses in a pulse train starting at  $t = 0$  that arrive at intervals of exactly one Larmor period cause rotations around the same axis, which we define as the  $x$  axis. Pulses delayed by one fourth or one half of the clock period will have a phase difference of  $\pi/2$  or  $\pi$ , causing rotations about the  $y$  axis or  $-x$  axis, respectively (Fig. 3). This sequence of three pulses can occur in less than the inverse Zeeman frequency, and thus for a reasonable Zeeman splitting of 100 GHz, an arbitrary single-qubit gate can be implemented in 10 ps.

To evaluate the importance of terms neglected in our approximate analysis, we numerically solve Eq. (2) as a three-state system driven by the classical field  $\Omega_1(t)$  using adaptive Runge-Kutte techniques. We use the realistic quantum-dot parameters  $\Gamma = (200 \text{ ps})^{-1}$  [22],  $T_2 = 10 \mu\text{s}$  [5,23], and  $\delta = 100 \text{ GHz}$ . We assume a Fourier-transform-limited Gaussian pulse detuned by 10 THz with a 100 fs full width half maximum. Using the definition of fidelity  $F = \langle \psi | \rho | \psi \rangle$ , where  $|\psi\rangle$  is the desired quantum state, we find it is possible to implement both  $\pi$  and  $\pi/2$  pulses with a fidelity  $F > 0.999$  (applied pulse energy densities of  $14 \mu\text{J}/\text{cm}^2$  and  $5 \mu\text{J}/\text{cm}^2$ , respectively, which is within the energy output of mode-locked semiconductor lasers followed by optical amplifiers). The fidelity as a

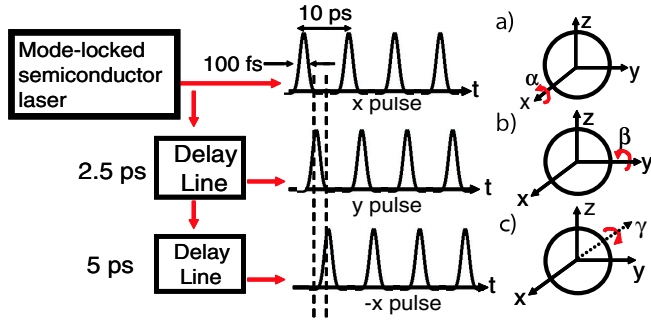


FIG. 3 (color online). Rotations about various axes induced by pulse delays, (a)  $x$ -pulse train (b)  $y$ -pulse train, and (c)  $-x$ -pulse train.

function of Rabi frequency (at the optimal detuning) is shown for both  $\pi$  and  $\pi/2$  pulses in Fig. 4(a). The general shape of the curve is increasing with Rabi frequency, as larger Rabi frequencies allow for larger detunings and therefore excite less population into the excited state. There are also some oscillations visible in the curve that are related to Rabi oscillations as the system finds optimum detuning regions. The high fidelity of the single-pulse Raman rotation is due to the speed of the pulse; all relaxation and decoherence processes occur at a time scale much slower than the pulse time.

For two-qubit gates implemented via the “qubus” concept, the single-mode cavity is driven by a narrow-band coherent-state pulse. We assume  $\delta \gg \Delta g^2 |\alpha|^2 / (4\Delta^2 + \Gamma^2)$ , where  $\alpha$  is the coherent-state amplitude and  $g$  is the vacuum Rabi splitting of the microcavity system. With this assumption, the Hamiltonian is nearly diagonal and there is negligible population change to the qubit. According to perturbation theory, the dominant correction term is the first-order diagonal correction found in the rightmost term of Eq. (3). This term describes an effective Hamiltonian of the form  $JS^z a^\dagger a$ , with  $J = \delta g^2 / (4\Delta^2 + \Gamma^2)$ . This interaction varies the phase of the coherent-state field depending on the spin-state of the quantum dot. Quantum logic is implemented by interspersing these optical phase shifts with optical displacements achieved by mixing the coherent-state pulse with a reference pulse at the optical switch. Assuming fast, accurate control of the switching ratio as well as the timing and phase of the reference

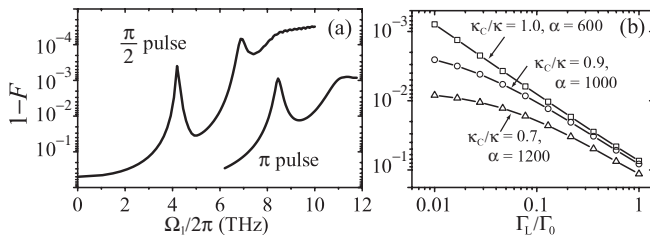


FIG. 4. (a) Fidelity of single-qubit rotations for  $\pi$  and  $\pi/2$  pulses vs Rabi frequency. (b) Fidelity of two-qubit gates vs  $\Gamma_L/\Gamma_0$  for different values of  $\kappa_c/\kappa$  and  $\alpha$ .

pulses, the amplitude of the coherent state may be taken through a closed path in phase space. The area of this path, and the resulting geometric phase, depends on the states of the two qubits interacting with the field, allowing a controlled-phase gate. Such a gate is deterministic and does not require detection or feedback. For details, see Ref. [8].

The magnitude of the conditional-phase shift depends on the detuning  $\Delta$  and the coherent-state amplitude  $\alpha$ . If  $\Delta$  is too small compared to  $g^2/\delta$ , there is insufficient selectivity between the two levels. If  $\Delta$  is too large, the magnitude of  $J$  becomes too small compared to decoherence processes. Increasing  $\alpha$  increases the phase shift, but if  $\alpha$  is too large then decoherence due to spontaneous emission and cavity losses becomes stronger.

To verify the magnitude and fidelity of the phase-shift operation as a function of  $\Delta$  and  $\alpha$ , we performed simulations of the interaction described by Eq. (2). Although the fully connected  $\Lambda$  system employed in this Letter is different from the asymmetric  $\Lambda$  system considered in Ref. [24], the effective Hamiltonian  $JS^z a^\dagger a$  is the same, and thus many of the qualitative conclusions apply. Unlike Ref. [24], however, quantitative calculations for the present proposal require a fully quantum-mechanical description of the cavity field, because the previous semiclassical approach fails when pulses are too fast. For our simulations, we use a basis of displaced Fock states,  $D(\alpha)|n\rangle$ , where  $D(\alpha) = \exp(\alpha a^\dagger + \alpha^* a)$ . If a conditional phase shift  $\vartheta$  occurs, the quantum dynamics may be simulated by a space of approximately  $|\alpha\vartheta|$  of these states ( $|\alpha\vartheta| = \sqrt{\pi}/2$  for qubus logic). We use more states than needed in the calculation to assure numerical accuracy. For these calculations,  $\Omega_1(t) = gS(t)a$ , where  $S(t)$  is the convolution of the input pulse shape with the filter function of the cavity [24]. Spontaneous emission in the cavity mode may leak into both the waveguide, with rate  $\kappa_c$ , and to lossy modes or absorption, with rate  $\kappa - \kappa_c$ . The decay rate  $\Gamma$  is now taken as the rate of spontaneous emission into noncavity modes,  $\Gamma_L$ , plus emission into the cavity mode that is lost, so  $\Gamma = \Gamma_L + (1 - \kappa_c/\kappa)F(\Delta)\Gamma_0$ , where  $\Gamma_0$  is the decay rate of the dot in the absence of the cavity [taken to be  $(200 \text{ ps})^{-1}$ ], and  $F(\Delta) \ll 1$  is the Purcell factor at high detuning. For our simulations, we assume a modest cavity  $Q$  of 1000 and a cavity mode volume of one cubic wavelength inside the semiconductor, typical parameters for semiconductor microcavities [25].

The simulations start with the system in the superposition state  $(|0\rangle + |1\rangle)/\sqrt{2} \otimes |\psi_I\rangle$ , where  $|\psi_I\rangle$  is the initial state of the coherent-state optical pulse. The fidelity is then calculated as the overlap of the final density matrix with some pure state  $(|0\rangle|\psi_0\rangle + |1\rangle|\psi_1\rangle)/\sqrt{2}$ , where  $|\psi_j\rangle$  are different optical states. We find that Gaussian pulses with root-mean-square width much shorter than 20 ps cause these optical states to vary significantly from the desired phase shifted coherent states. However, for 20 ps pulses and with detunings of  $\Delta = 4 \text{ THz}$ , we are able to find

values of  $\alpha$  large enough to assure coherent states shifted by  $|\alpha\vartheta| = \sqrt{\pi/2}$ . We find that the final-state fidelity depends on the cavity figures of merit  $\Gamma_L/\Gamma_0$  and  $\kappa_c/\kappa$ , as shown in Fig. 4(b). If  $\Gamma_L/\Gamma_0 = 0.1$ , a value consistent with existing photonic crystal cavities [25], the fidelity may reach 99.3%. The fidelity may also be improved by increasing the pulse length, increasing the  $Q$ , or decreasing the mode-volume of the cavity. The fidelity of the final gate also depends on optical loss in the waveguide. The analysis in Ref. [24] indicates that the percent reduction of gate fidelity is about equal to the percent amount of loss, and it will therefore be a critical parameter to optimize when designing a fault-tolerant architecture.

The time required for two-qubit gate operations is limited by the pulse width and the pulse propagation time between qubits. Nonlocal two-qubit gates will therefore take just a few periods of the 100 GHz system clock. To allow gates between arbitrary qubits, qubits must be switched “on” and “off” with respect to their coupling to the probe pulse field. In the schematic of Fig. 1, it is supposed that each cavity is far off resonant from the probe pulse field so that the qubit is off with respect to light-mediated two-qubit gates. To switch the interaction on for a particular dot, a powerful, midband light source is focused on the cavity of interest to quickly tune it to resonance with the probe pulse (but still detuned by  $\Delta$  from the dot) via the optical Kerr nonlinearity.

Several features of this scheme favor scalability. The ability to achieve two-qubit gates between distant qubits is a key advantage, since schemes relying on nearest-neighbor interactions have more difficulty achieving fault-tolerant operation [26]. Another advantage of our approach is that the two quantum dots participating in two-qubit gates need not have the same frequency; several THz inhomogeneity is tolerated, easing the possibility of large-scale fabrication. Multiple rings of qubits could be integrated on a single chip and operated in parallel. Fast measurement of the qubits could be accomplished by the same conditional phase shifts of bright coherent pulses, which can be measured via homodyne detection with ordinary photodetectors.

One technical challenge is presented by the  $g$ -factor inhomogeneity of quantum dots. This inhomogeneity necessitates the use of spin-echo techniques to synchronize each qubit with the master clock. This technical burden may be relieved by using donor-bound excitons instead, as these impurity transitions form the needed  $\Lambda$  transition but show improved  $g$  homogeneity [27,28].

In summary, we have outlined a proposal for performing ultrafast, optically controlled quantum gates on electron spins in quantum dots using stimulated Raman scattering and qubit-controlled phase shifts with single optical pulses. For the single-qubit rotations, the optical pulses have a bandwidth large compared to the splitting of the two lower  $\Lambda$  states; for two-qubit gates the pulses must have a narrower bandwidth, but may still be as short as 20 ps. The

timing of the optical pulses is precisely controlled to provide the system’s clock signal and control the qubit rotation axis. The clock speed of a single-qubit gate in this scheme is limited only by the lower state splitting. These methods provide the basis for an ultrafast, scalable, solid-state, electron-spin based, all-optical quantum computer.

The authors thank H. Wang, S.E. Harris, K. Nemoto, W. Munro, and D. Press for helpful discussions. S. Clark received partial support from HP through the Center for Integrated Systems. This work was financially supported by the MURI Center for photonic quantum information systems (ARO/ARDA Program No. DAAD19-03-1-0199), JST/SORST program for the research of quantum information systems for which light is used, University of Tokyo (CINQIE) Special Coordination Funds for Promoting Science and Technology, and the “Qubus quantum computer program” MEXT, NII.

---

\*sclark4@stanford.edu

- [1] M. A. Nielsen and I. L. Chuang, *Quantum Computation and Quantum Information* (Cambridge University Press, Cambridge, England, 2000).
- [2] D. Loss and D. P. DiVincenzo, Phys. Rev. A **57**, 120 (1998).
- [3] R. Vrijen *et al.*, Phys. Rev. A **62**, 012306 (2000).
- [4] L. Childress *et al.*, Phys. Rev. Lett. **96**, 070504 (2006).
- [5] J. R. Petta *et al.*, Science **309**, 2180 (2005).
- [6] A. Imamoglu *et al.*, Phys. Rev. Lett. **83**, 4204 (1999).
- [7] C. Piermarocchi *et al.*, Phys. Rev. Lett. **89**, 167402 (2002).
- [8] T. P. Spiller *et al.*, New J. Phys. **8**, 30 (2006).
- [9] W. Yao, R.-B. Liu, and L. J. Sham, Phys. Rev. Lett. **95**, 030504 (2005).
- [10] S. E. Economou *et al.*, Phys. Rev. B **74**, 205415 (2006).
- [11] M. V. G. Dutt *et al.*, Phys. Rev. B **74**, 125306 (2006).
- [12] D. Suter and J. Mlynek, Phys. Rev. A **43**, 6124 (1991).
- [13] Z. Kis and F. Renzoni, Phys. Rev. A **65**, 032318 (2002).
- [14] D. Meshulach and Y. Silberberg, Nature (London) **396**, 239 (1998).
- [15] N. Dudovich, D. Oron, and Y. Silberberg, Nature (London) **418**, 512 (2002).
- [16] Y. Wu *et al.*, Physica (Amsterdam) **25E**, 242 (2004).
- [17] J. I. Cirac *et al.*, Phys. Rev. Lett. **78**, 3221 (1997).
- [18] M. D. Lukin, S. F. Yelin, and M. Fleischhauer, Phys. Rev. Lett. **84**, 4232 (2000).
- [19] L.-M. Duan *et al.*, Phys. Rev. Lett. **85**, 5643 (2000).
- [20] K. Sato, Electron. Lett. **37**, 763 (2001).
- [21] D. Gammon *et al.*, Science **273**, 87 (1996).
- [22] J. Hours *et al.*, in *Physics of Semiconductors: 27th International Conference on the Physics of Semiconductors* (Springer, New York, 2005), p. 771.
- [23] A. Greilich *et al.*, Science **313**, 341 (2006).
- [24] T. D. Ladd *et al.*, New J. Phys. **8**, 184 (2006).
- [25] D. Englund *et al.*, Phys. Rev. Lett. **95**, 013904 (2005).
- [26] K. M. Svore, B. M. Terhal, and D. P. DiVincenzo, Phys. Rev. A **72**, 022317 (2005).
- [27] V. A. Karasyuk *et al.*, Phys. Rev. B **49**, 16381 (1994).
- [28] K.-M. C. Fu *et al.*, Phys. Rev. Lett. **95**, 187405 (2005).